Conference Paper, Published Version

Umeda, Shinya; Yamazaki, Tatsuo; Ishida, Hajime

Time Evolution of Scour and Deposition around a Cylindrical Pier in Steady Flow

Fourth International Conference on Scour and Erosion 2008

TIME EVOLUTION OF SCOUR AND DEPOSITION AROUND A CYLINDRICAL PIER IN STEADY FLOW

Shinya UMEDA[1],Tatsuo YAMAZAKI[2], Hajime ISHIDA[3]

[1]Member of JSCE, Lecturer, Division of Civil and Environmental Eng., Kanazawa University
(Kakuma-machi, Kanazawa, Ishikawa, 920-1192, Japan)
E-mail: umeda@t.kanazawa-u.ac.jp
[2]Graduate studenet, Division of Civil and Environmental Eng., Kanazawa University
(Kakuma-machi, Kanazawa, Ishikawa, 920-1192, Japan)
E-mail: usui0420@yahoo.co.jp
[3]Member of JSCE, Professor, Division of Civil and Environmental Eng., Kanazawa University
(Kakuma-machi, Kanazawa, Ishikawa, 920-1192, Japan)
E-mail: hishida@t.kanazawa-u.ac.jp

Laboratory experiments were conducted on the time evolution of clear water scour around a cylindrical pier in steady flow. Three-dimensional topography of the scour and deposition is carefully measured using digital stereo-photogrammetry as a method to level the sand surface. The results show the scour pattern varies in developmental stages of scour and the scouring process is coupled to vortex flow and sediment transport. A deep scour hole and low mound of deposited sediment appear around the pier in a fine sand bed. The final scour depth is about 1.3 times the pier diameter. The final eroded volume at the pier is about 14 times the cube of the pier diameter, while the final deposited volume behind the pier is about 5.5 times. The rest of the eroded volume at the pier is transported as suspended load to downstream of the sediment mound. The ratio of the deposition to the erosion fluctuates in the range of 0.4 to 0.6 during the scour process.

Key Words : *pier,clear water scour,sediment transport,scour volume,stereo-photogrammetry*

1. INTRODUCTION

Scour around the foundations of river and marine structures is one of the major causes of serious damage to such structures. Considerable understanding of flow and scour around a cylindrical pier has been achieved by a great many experimental research works over a long time (e.g. Whitehouse[1)], Melville and Coleman[2)]; Sumer and Fredsoe[3)]). Based on this knowledge, attempts have been made to mathematically model scour over the last two decades (e.g. Richardson and Panchang[4)], Rouland et al.[5)]; Umeda et al.,[6)]). However, mathematical methods are still not sufficiently developed to be reliable as tools for engineering use because of the inherent complexities of scour phenomena, including the combined effects of three-dimensional separated flow, interaction of the flow field and sediment transport, and time-dependent scour patterns. Further experimental investigations concerning the basic mechanism of scour are needed for a deeper understanding of these effects. Although there have been many experimental and analytical studies on the formulation of scour depth equations, only a few studies have described the three-dimensional topography of scour and its time evolution. Little is known about the effect of time on the scour and deposition patterns, which are connected with time-dependent flow and sediment transport.

The purpose of the present study is to clarify the time evolution of the three-dimensional topography of scour and deposition around a cylindrical pier under a clear-water condition. Detailed descriptions are given of the scour process in conjunction with vortex flows and sediment transport. The effects of time on the development of scour depth and scour and deposition volumes are carefully investigated by means of topographic measurements using digital stereo-photogrammetry. These research results may be useful in the calibration of a mathematical scour model as well as for understanding the scour mechanism.

2. EXPERIMENTAL SETUP AND MEASURING TECHNIQUE

Experiments were carried out in a flume 12 m in length, 0.4 m in width, and 0.4 m in depth [see **Fig. 1**]. The flume had a mild slope of 1/1000. Flow was steady and comes from the left in Figure 1. A vinyl chloride cylinder was used as a pier model with an outside diameter D = 32 mm. The cylinder was installed in a 0.135 m deep sediment recess filled with fine sand. The sand grains had a mean size of d_{50} = 0.139 mm, a uniformity coefficient of d_{60}/d_{10} = 1.78 and a specific gravity of 2.65. Scouring tests were performed under a clear water scouring condition. The mean water depth on the initial plane bed was 0.146 m for a water discharge Q = 9.985 L/s. The average velocity of the approaching flow was U_0 = 0.171 m/s. The Froude number was F_r = 0.14. The pier Reynolds number was Re_p = 4560. The tests were run for 10.3 hours until the variation in the scour depth was less than 1 mm in 1 hour. However, it is necessary to run tests for several more days to achieve an equilibrium condition for the clear water scour (cf. Melville and Chiew[7]). The present study is focused on the early developmental stages of scour. We conducted the scouring test several times for the same condition.

The topography of the scoured sand bed was leveled by digital stereo-photogrammetry. This technique is essentially based upon the concept of triangulation, in which three-dimensional object points can be determined from corresponding image points from at least two perspectives. This technique can determine sand bed elevations around the cylindrical pier. Four perspectives shown in **Fig. 2** were taken from different directions to provide four stereo-pairs of images, i.e. **Fig. 2** (a)-(b), (c)-(d), (a)-(c) and (b)-(d), for accurately estimating the bed geometry near the pier base. After draining water from the flume, images were taken with a 10.2-megapixel digital camera fitted with a 30 mm lens. While the object distance from the lens focal point was about 0.7 m, the base distance of focal points for each stereo-pair of images ranged from 0.2 m to 0.5 m. Under this condition, the images cover an area of 0.6 m x 0.4 m. Images were taken of the sand bed together with many pass points on rulers to have more than five pass points in each stereo-pair of images. These images were analyzed with Topcon stereo-photogrammetric software.

To validate the accuracy of the stereo-photogrammetric system, initial tests were carried out for the simple geometry model shown in **Fig. 3**. The scale of the model is as large as that of the scour

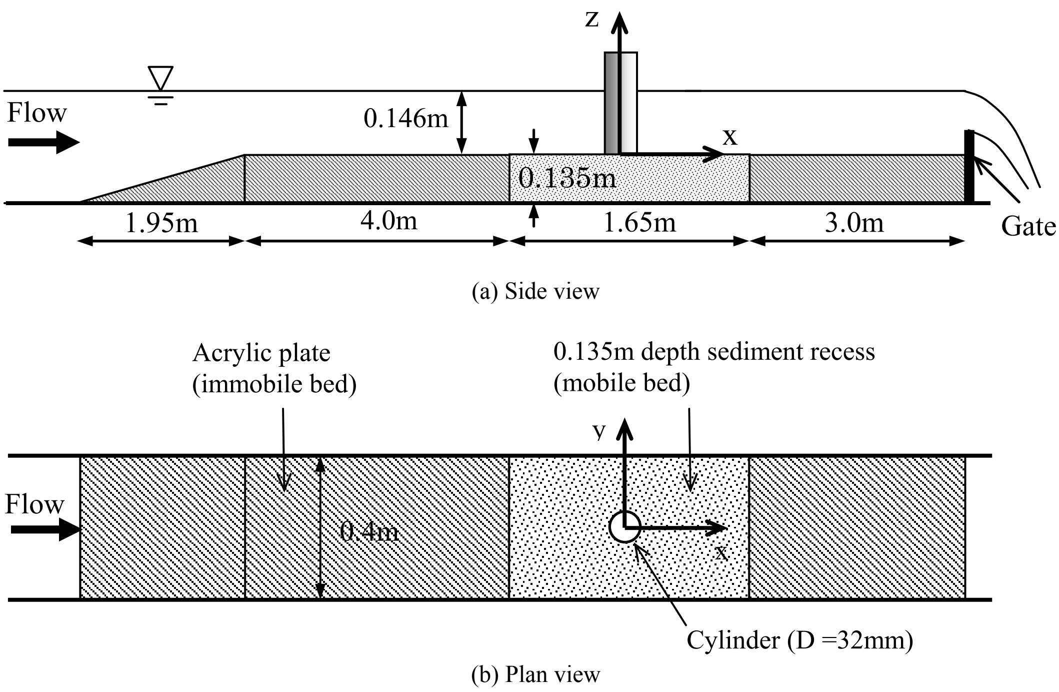

(a) Side view

(b) Plan view

Fig. 1 Experimental arrangement in the flume

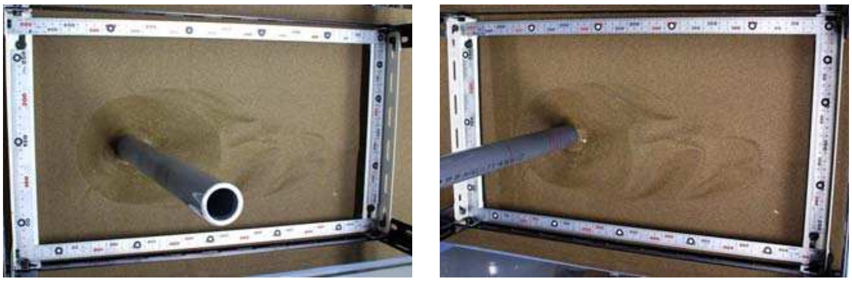

(a) Upstream left side (b) Downstream left side

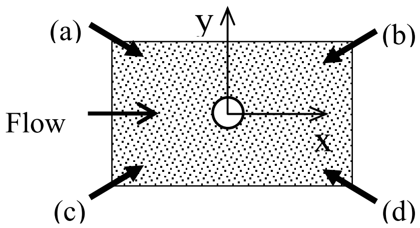

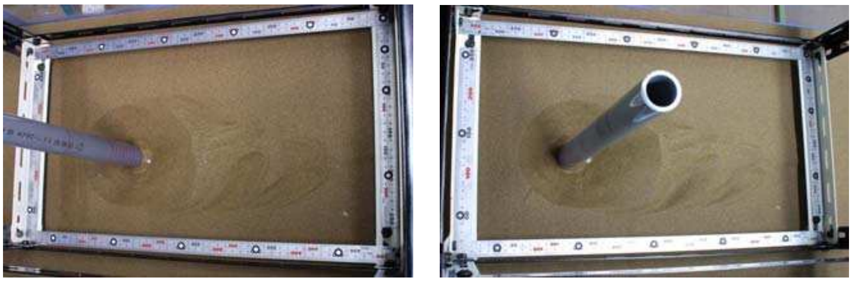

(c) Upstream right side (d) Downstream right side

Fig. 2 Stereo-pairs of images of the sand bed around the cylindrical pier

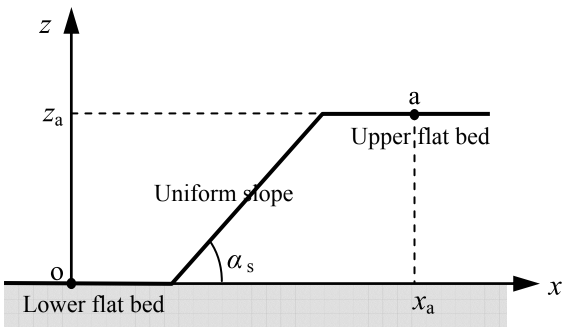

Fig. 3 Geometry of model to validate the stereo-photogrammetry system

Table 1 Initial validation of the stereo-photogrammetric system

	Estimation (A)	Measurement (B)	Absolute error (C = |A-B|)	Rate of error (D = C/A)
Horizontal dimensions x_a [mm]	226.85	227.00	0.15	0.0007
	356.80	357.00	0.20	0.0006
Vertical dimensions z_a [mm]	4.93	5.05	0.12	0.0238
	10.30	10.20	0.10	0.0098
	15.20	15.50	0.30	0.0194
Slope angle α_s [degree]	30.21	30.0	0.21	0.0070
	45.76	45.0	0.76	0.0169
	59.86	60.0	0.14	0.0023

tests. The object distance and base distance were about 0.8 m and 0.3 m, respectively. **Table 1** shows the comparison between the dimensions estimated by the photogrammetry system and the dimensions measured by rulers and set squares. Table 1 suggests the photogrammetry system can determine the horizontal and vertical coordinates of each object point with high accuracy. The accuracy of estimating the horizontal coordinates is much better than that of estimating the vertical coordinates. The system can estimate the vertical coordinates with an accuracy of better than 1 mm. It was also found the system was adaptable to estimating the slope angle and slope profile with high accuracy.

3. GENERAL PATTERN OF SCOUR AND DEPOSITION

Figure 4 shows the three-dimensional bed topography around the pier 620 minutes after the beginning of the scour. The negative elevation of the sand bed is denoted by dotted contour lines in **Fig. 4** (b). While a deep scour hole develops around the pier, a low mound of deposited sediment appears in the wake region. The maximum scour depth and maximum deposition height normalized with the pier diameter reach 1.3 and 0.7, respectively. The scour hole is an inverted and truncated cone in shape and the sediment mound is a crescent in shape. Sand ripples are also formed on the downstream side of the sediment mound. The ripples and sediment mound continuously move and enlarge during the scour test.

The longitudinal and cross sections of the scour hole in **Fig. 4** are shown in **Fig. 5**. From video images, patterns of sediment transport in the scour hole were sketched in the figure. The scour hole is steeper upstream of the pier. Although two depressions form on the upstream slope of the scour hole [see a-b and b-c in **Fig. 5** (a)], the scour hole has a 33 degree slope on average. The local slope angle reaches about 39 degrees in the upper depression. This angle corresponds to an angle of repose above which the sediment slides downward. The horseshoe vortex in front of the pier continues to lift sediment, which is partly eroded from the lower depression b-c and partly supplied by the sliding of sediment on the upper depression a-b. The lifted sediment is transported downstream from peak b joining the two depressions as suspended load. This scour pattern upstream of the pier is consistent with the experimental observation of Dargahi[8)] for clear water scour.

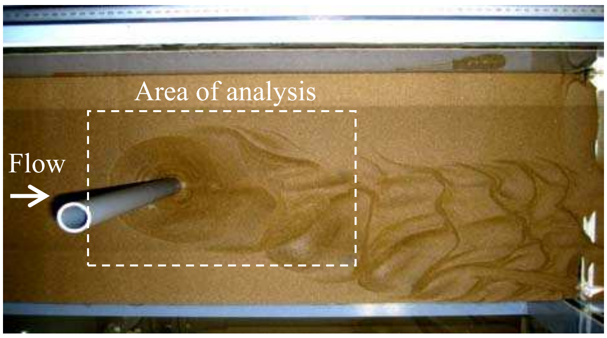

(a) photography of the sand bed

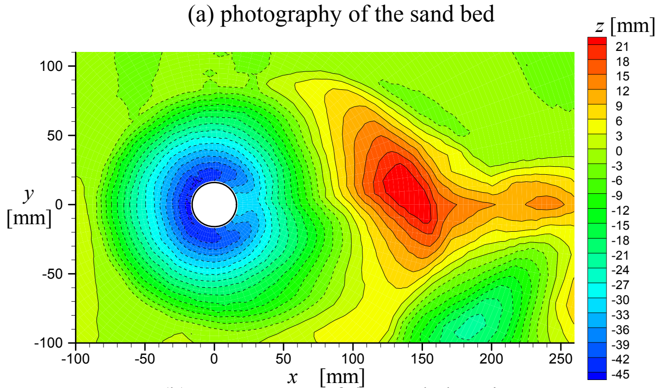

(b) contour map of the sand elevation

Fig. 4 Three-dimensional bed topography around the cylindrical pile 620 minutes after the beginning of the scour

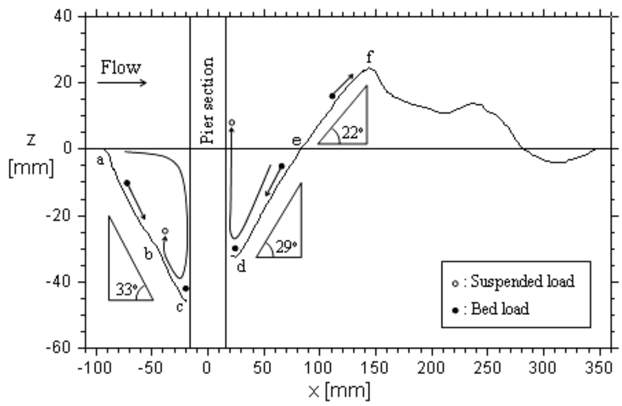

(a) longitudinal section

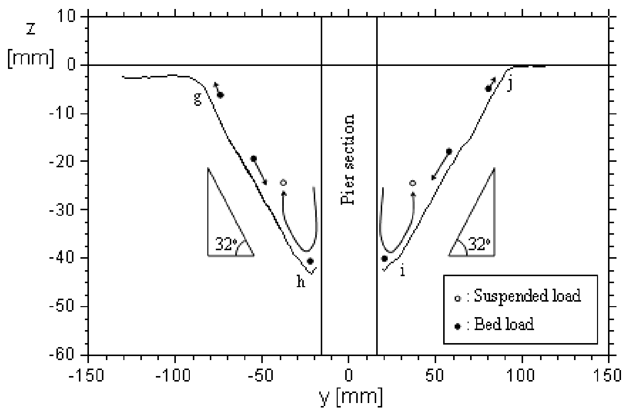

(b) cross section

Fig. 5 Scour profiles at 620 minutes and a sketch of sediment transport

We find in **Fig. 5** (b) that the scour hole at the sides of the pier has a profile similar to the upstream scour hole, but the side scour is relatively shallow. Although the sediment on the side slope is partly picked up by the horseshoe vortex, the rest is transported downstream as bed load. The former pass the sediment mound, but the latter is fed into the mound. Consequently, the side scouring leads to the sediment mound downstream of the pier. The magnitude of the sediment mound depends on the volume of the sediment swept by the contraction of flow. The sediment mound has a 22 degree front slope on average [see e-f in **Fig. 5** (a)]. This slope is milder than that of the lower slope d-e. While the sediment continuously slides upward on the upper slope e-f, the sediment slides downward on the lower slope d-e. The wake vortices continue to pick up the downward sliding sediment near the pier base, and then the sediment is transported downstream as suspended load. The suspended sediment is diffused by time-dependent flow in the wake, but the suspended sediment is finally deposited on a broad bed in the downstream direction.

4. TIME EVOLUTION OF SCOUR AND DEPOSITION

Figure 6 shows the time evolution of the bed topography during scour development. The scour starts at the shoulders of the pier, and then the scouring enlarges to the surrounding area. In the initial stage of scour, there are two small depressions expanding from the pier shoulders to the downstream. Since some of the eroded sediment drifts downstream along the pier base, the deposition of the sediment occurs behind the pier base. The flow accelerated by the contraction of the main flow continues to sweep volumes of sediment into the sediment mound. The sediment mound is significant 10 minutes after the beginning of scour. Sand ripples then appear downstream of the mound. As the scouring enlarges, the scour hole upstream of the pier becomes an inverse truncated cone in shape. After 10 minutes, the shape of the scour hole is maintained during further scour development. This is in agreement with findings in several other works (e.g. Yanmaz and Altinbilek[9]). Although the initial scour is mainly induced by the combined action of the horseshoe vortex and flow contraction, the vortex shedding in the wake also plays an important role in the development of the scour hole as the scour progresses. After a few minutes when the sand bed beside the pier is eroded to a certain depth [cf. **Fig. 6** (b)], the wake vortices trap and eject a large amount of sediment from the scour hole. Most sediment ejected by the wake vortices is transported from the rear of the pier base to far downstream of the sediment mound. The sediment transport is quasi-periodical due to the periodic motion of vortex shedding.

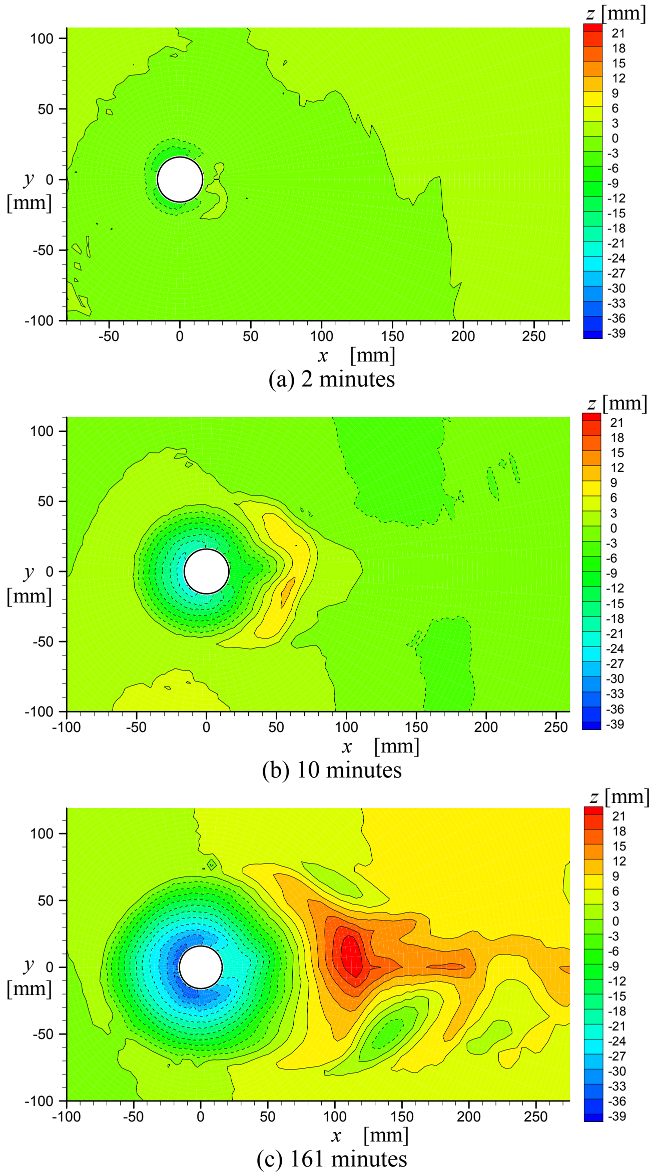

Fig. 6 Contour maps of the sand bed elevation during scour development

The time evolution of the normalized scour depths S/D upstream of the pier is shown in **Fig. 7**. From video images, the scour depths were measured at two points: the front edge and the shoulder of the pier base. The horizontal axis of the figure is time with respect to the duration of the test, t_e = 620 minutes. Almost one-half the final scour depth is achieved at about 0.06 of the test duration. The scour depths increase rapidly in the initial stage of the scour process, and then each equilibrium scour depth is generated gradually. The time variations of the scour depths approximately follow exponential curves. The final scour depth for the test is about 1.2, whereas the equilibrium scour depth will be deeper. The scour is deeper at the pier shoulder until t/t_e reaches approximately 0.4. As the scour progresses further, the scour becomes deeper at the front edge of the pier. In the later stage when the long adverse slope develops upstream of the sediment mound [cf. slope d-e-f in **Fig. 5** (a)], sediments near the sides of the pier base resist being eroded. This is because the toe of the sediment mound approaches the sides of the pier base.

Figure 8 shows the time evolution of scour and deposition volumes normalized with the cube of the pier diameter. The scour and deposition volumes correspond to the volume of the near-pier scour hole V_e and the volume of the prime sediment mound behind the scour hole V_d respectively. Like the scour depths, the scour and deposition volumes increase with time, but the rates of increase gradually decrease. While the normalized scour volume V_e/D^3 reaches about 14 at the end of the test, the deposition volume V_d/D^3 is 5.5. The difference between the two volumes (V_e-V_d) represents the volume of sediment transported downstream of the prime mound. It has been confirmed that the scour volume V_e/D^3=14 is in good agreement with V/D^3=13(+/−3) measured by Margheritini et al.[10] for live-bed scour. However, there is a possibility that the present value will increase until scour equilibrium is achieved. Except for the initial stage of scouring (t/t_e>0.01), the ratio of the deposition volume to the scour volume fluctuates in the range of 0.4 to 0.6. It is found the ratio V_d/V_e is highest at t/t_e = 0.25.

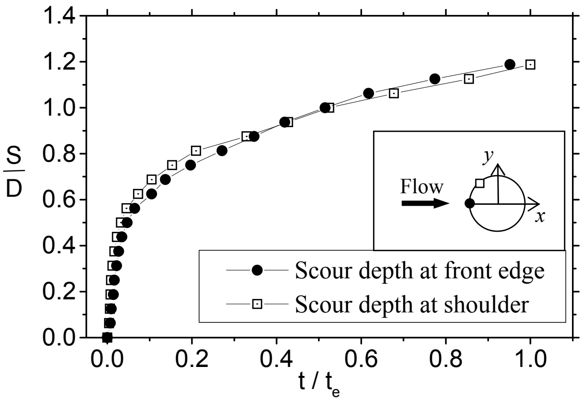

Fig. 7 Time variation of scour depth upstream of the pier (t_e = 620 minutes)

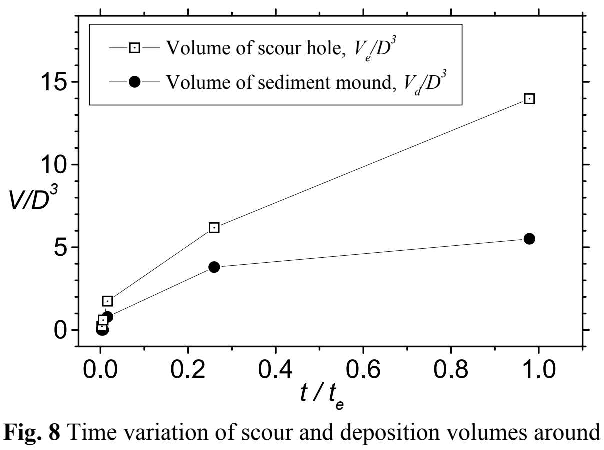

Fig. 8 Time variation of scour and deposition volumes around the pier (t_e = 620 minutes)

5. CONCLUSIONS

An experimental investigation was conducted on the time evolution of scour and deposition around a cylindrical pier in steady flow. The three-dimensional topography of scour hole was carefully measured by digital stereo-photogrammetry under a clear water condition. The main results obtained in this study are as follows.

A scour hole and sediment mound develop around a pier in a fine sand bed. The scour depth increases rapidly in the initial stage of the scour process. The time variation of the scour depth follows an exponential curve. Although the scour is deeper at the pier shoulder in an early stage of scour process, the scour becomes deeper at the front edge of the pier as the scour progresses further. When the bed beside the pier base is eroded to a certain depth, lee-wake vortices pick up and eject volumes of sediment from the rear of the pier base. While the initial scour is mainly induced by the combined action of the horseshoe vortex and flow contraction, the vortex shedding in the wake also plays an important role in enlargement of the scour hole as scour progresses. The final scour depth and deposition height reach 1.3 and 0.7 with respect to the pier diameter, respectively. The shapes of the scour hole and sediment mound are approximately an inverse truncated cone and a crescent, respectively.

Like the scour depths, the scour and deposition volumes increase with time and then the rates of increase gradually decrease. The final scour and deposition volumes reach about 14 times and 5.5 times the cube of the pier diameter, respectively. However, there is a possibility that the final volumes and scour depth will increase until scour equilibrium is achieved. The ratio of the deposition volume to the scour volume fluctuates in a range of 0.4 to 0.6.

ACKNOWLEDGMENT: The present work is partially supported by a Grant-in-Aid for Scientific Research (No. 19760335) from the Ministry of Education, Culture, Sports, Science and Technology,

Japan, for which we are grateful.

REFERENCES

1) Whitehouse, R. : Scour at Marine Structures. Thomas Telford Publications, UK, 198 pp, 1998.
2) Melville, B.W. and Coleman, S.E. : Bridge Scour. Water Resources Publications, USA, 550 pp, 2000.
3) Sumer, B.M. and Fredsoe, J. : The mechanics of scour in the marine environment, World Scientific Publishing, Singapore, 536 pp, 2002.
4) Richardson, J. E. and Panchang, V. G. : Three-dimensional simulation of scour-inducing flow at bridge piers, J. Hydraul. Engng., ASCE, Vol.124, pp.530–540, 1998.
5) Rouland, A., B. M., Sumer, J. Fredsoe and J. Michelsen. : Numerical and experimental investigation of flow and scour around a circular pile, J. Fluid Mechanics, Vol.534, pp.351-401, 2005.
6) Umeda, S. Cheng, L. Yuhi, M. and Ishida, H. : Three-dimensional numerical model of flow and scour around a vertical cylinder, Proc. of the 30th Int. Conf. Coastal Eng., ASCE, pp.2354-2366, 2006.
7) Melville, B.W. and Chiew, Y. : Time scale for local scour at bridge piers, J. Hydraulic Engineering, Vol. 125, No. 1, pp.59-65, 1999.
8) Dargahi, B. : Controlling mechanism of local scouring, Journal of Hydraulic Engineering, Vol. 116, No. 10, pp.1197-1214, 1990.
9) Yanmaz, A.M. and Altinbilek, D.A. : Study of time-dependent local scour around bridge piers, Journal of Hydraulic Engineering, Vol. 117, No.10, pp.1247-1268, 1991.
10) Margheritini, L. Martinelli, L. Lamberti, A. and Frigaard, P. : Scour around monopole foundation for off-shore wind turbine in presence of steady and tidal currents, Proc. of the 30th Int. Conf. Coastal Eng., ASCE, pp.2330-2342, 2006.